Efficient bionic nanozyme based on AuPt NPs@ZIF-90 used for cyclic catalysis multimodal tumor therapy

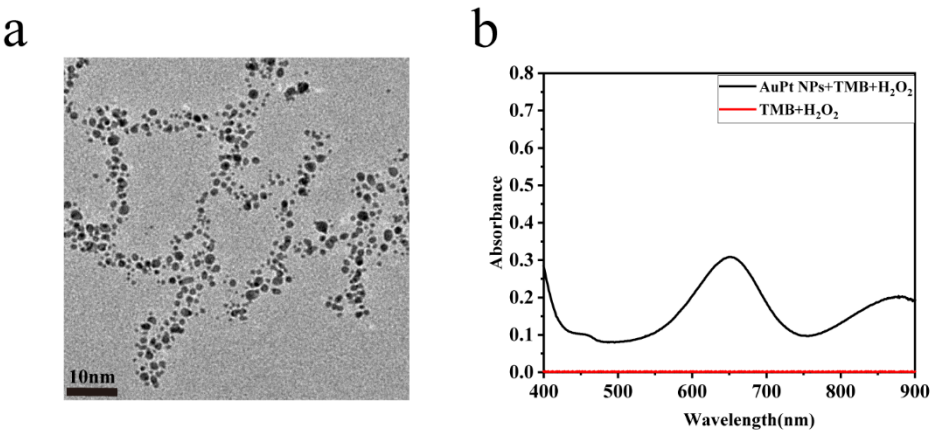

Figure S1 (a) TEM images of AuPt NPs;(b) POD enzyme activity assay of AuPt NPs;

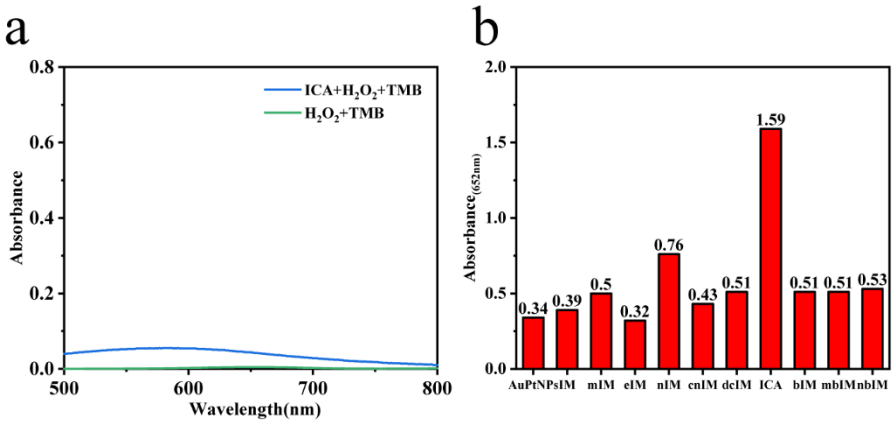

Figure S2 (a) POD enzyme activity assay of ICA; (b) UV absorption values of peroxidase activity at 652 nm by TMB after mixing of different imidazolylated small molecules with AuPt NPs;

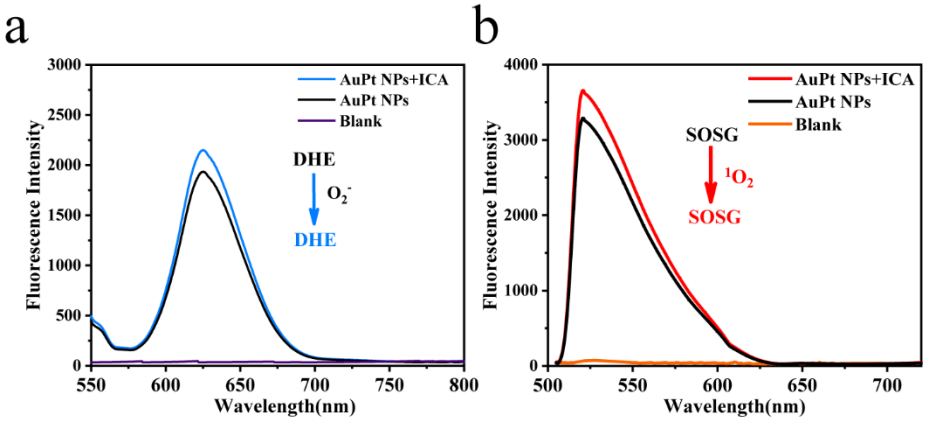

Figure S3 (a) The ability of AuPt NPs to produce $^1O_2$ before and after mixing with ICA was detected using the SOSG fluorescent probe; (b) The ability of AuPt NPs to produce O^{2-} before and after mixing with ICA was detected using the DHE fluorescent probe.

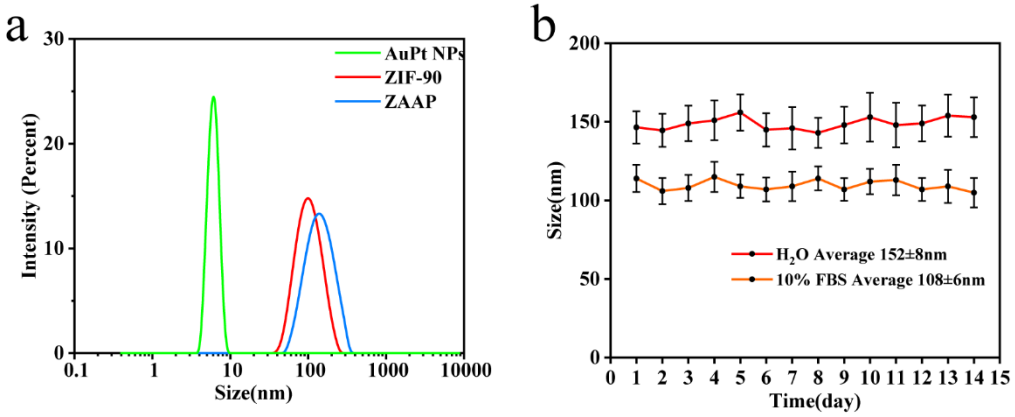

Figure S4 (a) Hydrated particle sizes of AuPt NPs, ZIF-90 and ZAAP; (b) Results of 15 days of monitoring of hydrated particle sizes of ZAAP in H_2O and FBS containing 10%, respectively, data expressed as mean ± standard deviation (n=3).

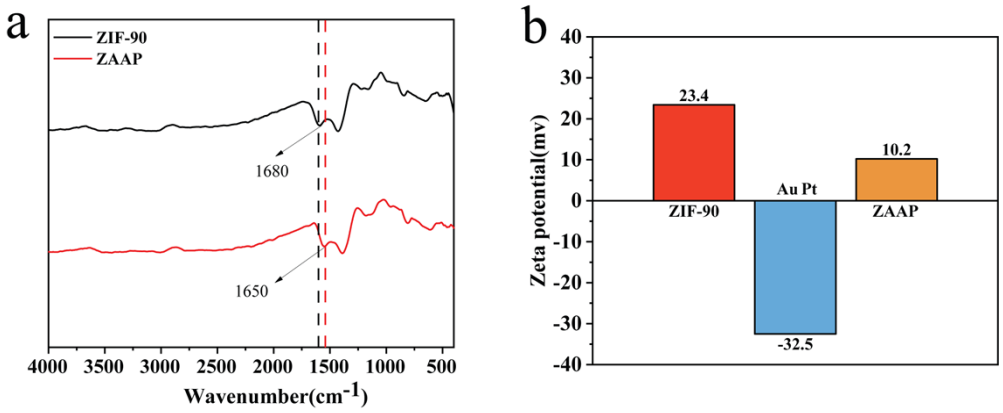

Figure S5 (a) ZIF-90 and ZAAP FTIR spectra; (b) Zeta potentials of AuPt NPs, ZIF-90 and ZAAP.

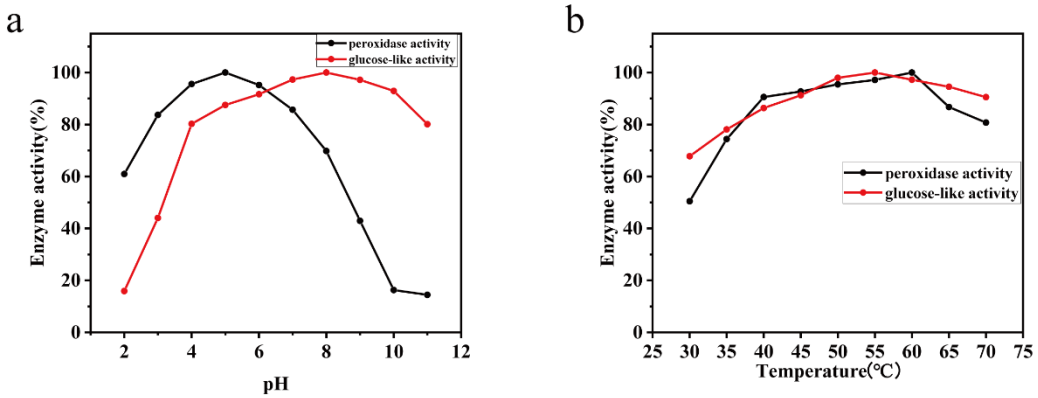

Figure S6 (a) Peroxidase and glucosidase-like activities of ZAAP change in activity over a pH of 2-11; (b) Peroxidase and glucosidase-like activities of ZAAP change in activity over 30-70°C;

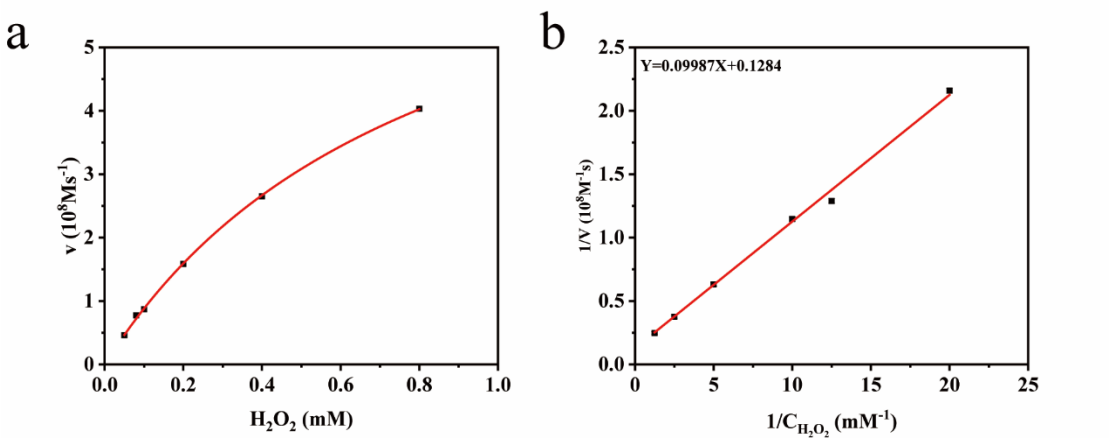

Figure S7 (a) POD enzyme activity assay of ZAAP, reaction rate equation when the catalytic substrate is H_2O_2; (b) Corresponding Michaelis constant equation fit.

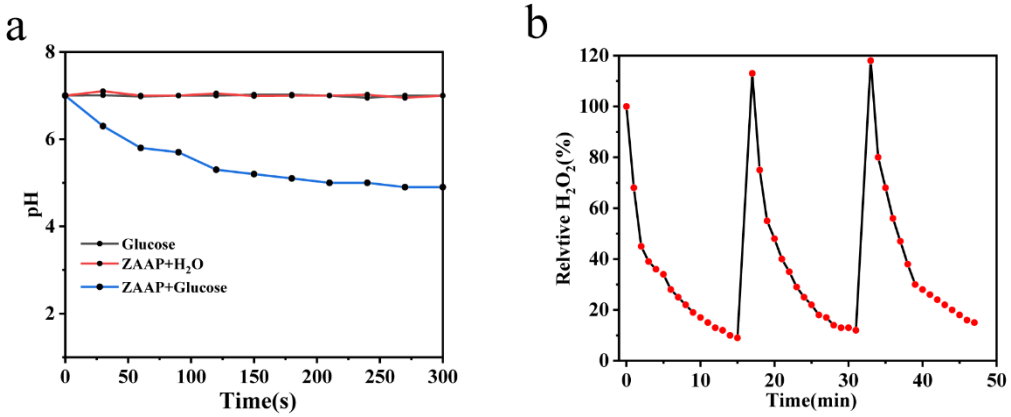

Figure S8 (a) Change in pH during 10 min of co-incubation of ZAAP with glucose; (b) Cycle of three experiments of ZAAP-catalyzed decomposition of H_2O_2.

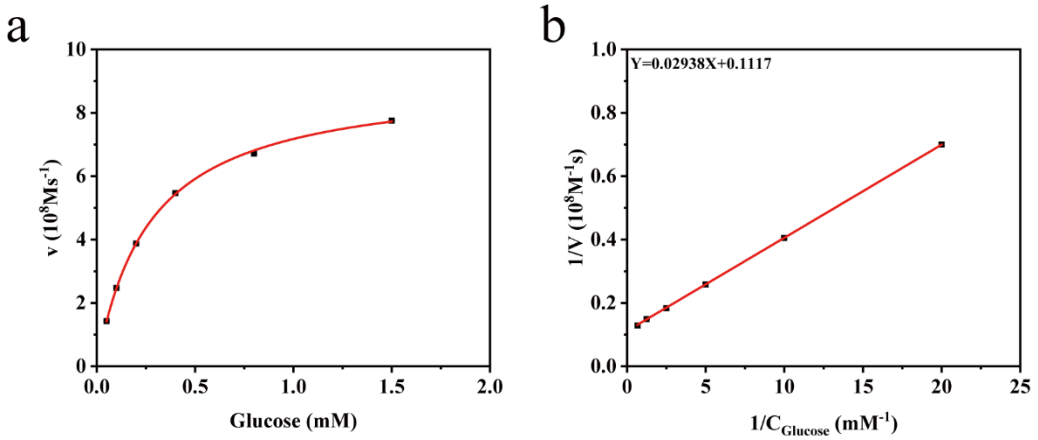

Figure S9 (a) GOD enzyme activity assay of ZAAP, reaction rate equation when the catalytic substrate is Glucose;(b) corresponding Michaelis constant equation fit.

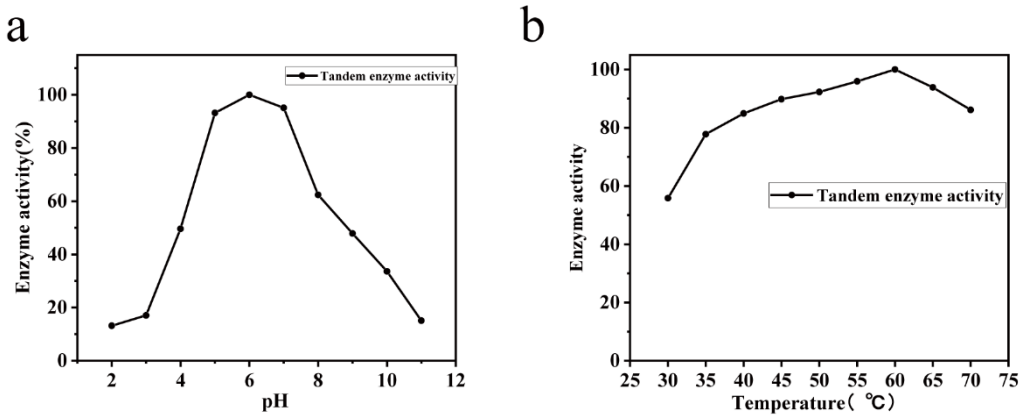

Figure S10 (a) Change in activity of POD and GOD tandem enzyme activities of ZAAP over 2-11 pH;(b) Change in activity of tandem enzyme activities of ZAAP over 30-70°C.

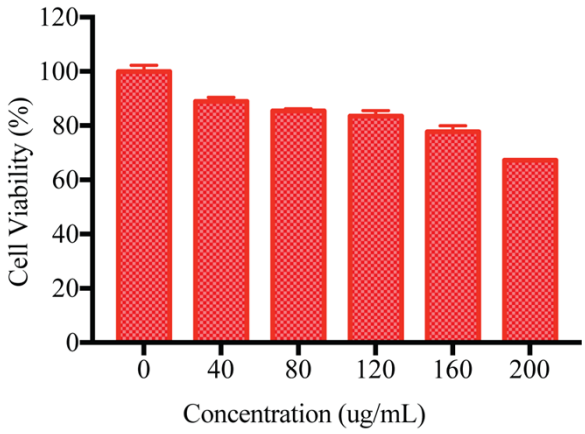

Figure S11 The cyto-toxicity of AuPt to 4T1 cells.

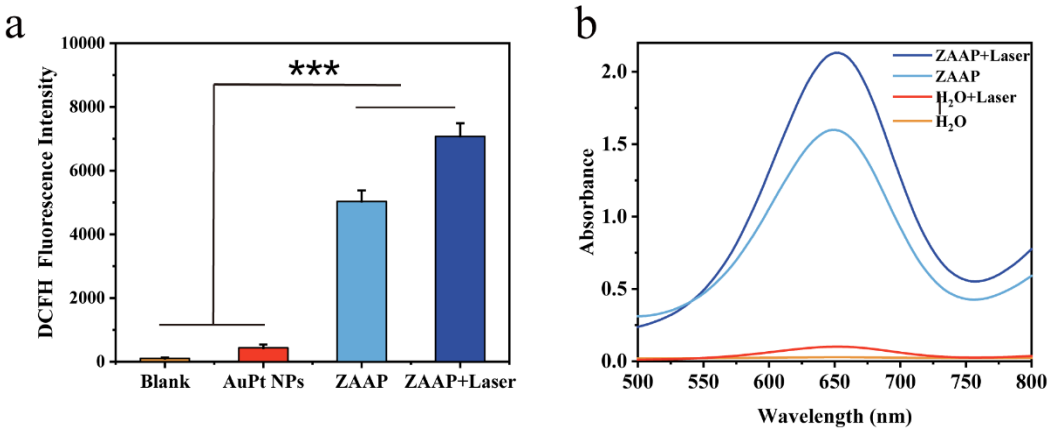

Figure S12 (a) Cytofluorescence images of ZAAP, AuPt NPs, and ZAAP+Laser induced 4T1 intracellular ROS production using DCFH-DA, data expressed as mean ± standard deviation (n=3) (analyzed for significance by t-test *p< 0.05, **p < 0.01, ***p < 0.001);(b) ZAAP in the presence or absence of 808 nm laser Comparison of the ability of ZAAP to catalyze the production of reactive oxygen species from H_2O_2 with and without 808 nm laser irradiation

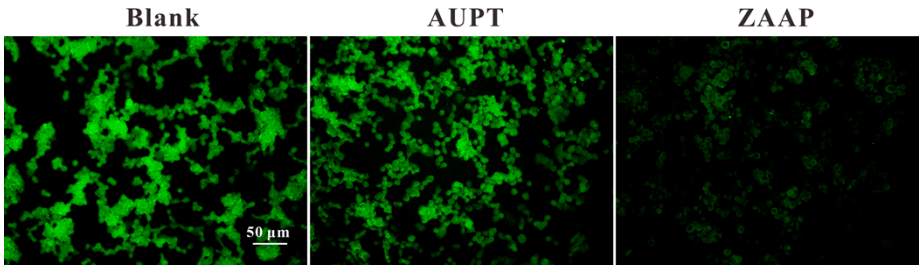

Figure S13 Oxygenation results in tumor cells incubated with blank, AuPt and ZAAP group.

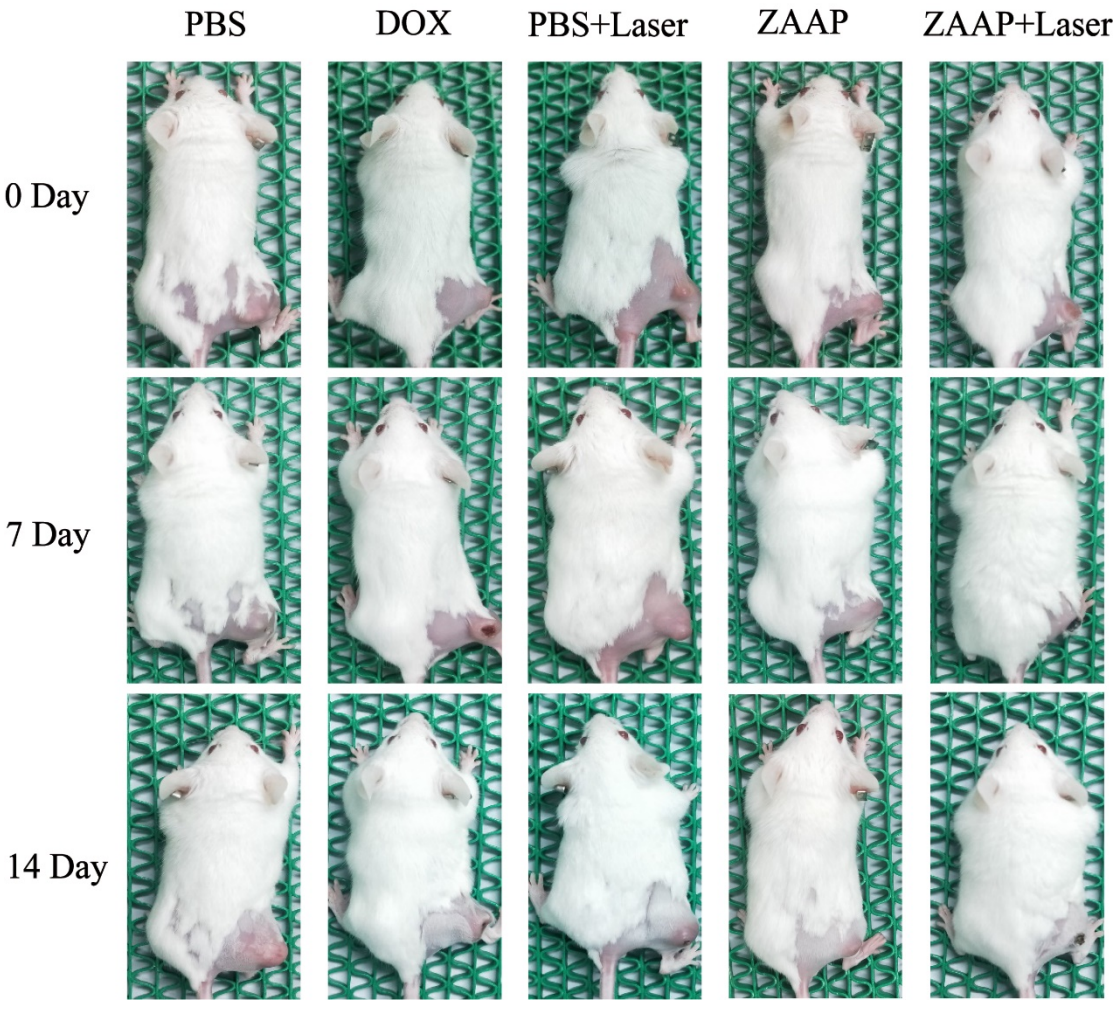

Figure S14 The treatment process of mice was observed at different time points (0, 7, and 14 days)

Table S1 Comparison of kinetic parameters for modeling enzyme activity

substrate / analog enzyme	K_m (mM)		V_{max} (10^{-8} M/s)	
	H_2O_2	Glucose	H_2O_2	Glucose
HRP	3.700		8.71	
GOX		4.87		6.9
ZAAP	0.835	0.268	8.19	9.09